Inorganica Chimica Acta 562 (2024) 121877

Contents lists available at ScienceDirect

Inorganica Chimica Acta

journal homepage: www.elsevier.com/locate/ica

Ab-initio electronic, magnetic, and optical properties of Fe-phthalocyanine on NiO(001)

Marco Marino [a,*], Elena Molteni [a], Simona Achilli [a], Guido Fratesi [a,*]

[a] ETSF and Physics Department "Aldo Pontremoli", University of Milan, via Celoria 16, Milano 20133, MI, Italy

ARTICLE INFO

Keywords:
Organic spintronics
Spinterface
Iron-phthalocyanine
NiO(001) surface
DFT +*U*
Optical spectroscopy

ABSTRACT

The adsorption of organic molecules on antiferromagnetic surfaces forms interfaces with potential applications in organic spintronics devices. Molecules modify the dispersion of spin excitations in the substrate through charge transfer and crystal deformations, and offer the possibility to couple them to light excitations. Here, we follow an ab initio approach to the study of the interface between the magnetic organo-metallic molecule Fe-phthalocyanine and the (001) surface of NiO. By applying Hubbard-corrected density-functional theory (DFT + *U*) calculations we determine the most stable adsorption configuration as that with the molecule lying flat with Fe above a surface O atom. We find a strong hybridization between Fe orbitals and surface ones, with the Fe spin coupled antiferromagnetically to subsurface Ni through the O atom. Moderate changes to the magnetic structure of the components and charge displacements are shown. Optical spectra show reduced absorption onsets and are investigated for the possibility of a coupling with the system spin properties.

1. Introduction

In the production of spintronics devices (i.e. systems combining spin and electronic degrees of freedom) [1], antiferromagnetic materials represent a reference point in the transport of high frequency (THz) coherent spin excitations [2–6] avoiding dissipative couplings with external magnetic stimuli [7]. In the subfield of organic spintronics [8,9], organic molecules can be adsorbed on substrates to modify interface properties and achieve mechanisms to produce spin excitations, while modifying their dispersion [10], so to obtain low energy-loss and light [11,12] and temperature [13] tunable spin-transport devices. The combination between molecules and substrates forms novel interfaces with peculiar properties which are the subject of the so-called "spinterface" physics [14–17].

On the substrate viewpoint, transition-metal (TM) oxides with high Neel temperature and insulating behaviour as the late transition-metal monoxides are valuable choices in order to build room-temperature spin-excitation transport devices [18]. In particular NiO has a Néel temperature of 525 K and a charge-transfer insulator character [19].

Among organic molecules, tetrapyrrolic organo-metallic molecules such as metal phthalocyanines [20,21] are optimal candidates for the formation of interface electronic and magnetic states, due to the tunability following the choice of the central metal (magnetic) core [22,23] in combination with the external organic macrocycle properties.

Many studies focused on the adsorption of metal-phthalocyanines on metallic surfaces [24] as copper[25], gold, silver and nickel [26], possibly passivated e.g. by a graphene layer to decouple the molecules from the strongly interacting metal, or on the graphene itself [27]. Particular attention is given to the dependence on the metal ionic centre, i.e. to the d orbital occupation, of the magnetic coupling between the molecule and the substrate or of the hybridization strength.

In the last years attention has also been given to the adsorption of these molecules on oxides, as In_2O_3 [28] and SrTiO [29], and TM-oxides, as TiO_x and MoO_x [30,31], CoO [32], MnO [33], focusing on structural deformations and charge-transfer mechanisms, with consequent filling/emptying of molecular orbitals. These complex systems also offer the possibility of spin-crossover effects [34] that can be induced through functionalization, i.e. with axial ligands on Cu(100) [35], or selecting the adsorption site, as in a N-doped graphene layer [36], or through light [37].

Similar phenomena were observed for other organo-metallic molecules. We mention studies of metal-tetraphenyl porphyrins adsorbed on metallic substrates, possibly passivated by O adlayers [38], exhibiting the possibility of spin-tuning through the functionalization with axial ligands [39–41], and of metal-porphyrins on ultrathin Co and Ni magnetic films on Cu(001) substrates, where films are partially oxidised to

* Corresponding author.
E-mail addresses: marco.marino1@unimi.it (M. Marino), guido.fratesi@unimi.it (G. Fratesi).

https://doi.org/10.1016/j.ica.2023.121877
Received 27 July 2023; Received in revised form 31 October 2023; Accepted 5 December 2023
Available online 9 December 2023

couple antiferromagnetically with the molecule [42], or of a Fe(II) complex on SiO_2 and Al_2O_3 dielectric substrates, spin-locked in a low-spin state and excited through light at temperatures beyond their typical spin-crossover temperature [43].

In this work, we study the interface between the magnetic Fe-phthalocyanine (FePc) molecule and antiferromagnetic NiO(001) by applying Hubbard-corrected density-functional theory (DFT + U) [44,19] calculations. We determine the adsorption configurations and investigate the electronic hybridization between molecular and surface states highlighting the changes to their magnetic structures. We further evaluate optical spectra of free and adsorbed molecules.

2. Computational Methods

The ground state and its properties are studied through a plane-waves Density Functional Theory (DFT) approach, as implemented in the Quantum ESPRESSO distribution [45,46]. We use the vdW-DF-C09 exchange–correlation (xc) functional [47,48], that includes van der Waals molecule-surface interactions. We apply the Hubbard correction in the Dudarev's formalism (a single parameter $U_{\text{eff}} = U - J$, denoted simply U in the following) to the d orbitals of the metal atoms (Ni and Fe), with $U_{\text{Ni}} = 4.0$ eV and $U_{\text{Fe}} = 5.0$ eV [49–52], to correct the self-interaction error which tends to de-localize the electrons. The value of U_{Ni} was chosen following Ref. [49] where the DFT $+U$ electronic density of states is matched to the many body GW one, to preserve the good alignment of O and Ni states in the bulk, at the cost of an underestimated gap. We compute a spin magnetic moment of Ni of 1.6 μ_B, in good agreement with previous theoretical calculations. That of U_{Fe} follows the choice of Ref. [52], in which a comparison between DFT + U and hybrid DFT calculations and experimental results is considered, taking into account electronic and structural properties. The Hubbard correction has been chosen in order to reproduce the Mott–Hubbard insulator character of NiO, and the low-magnetic state of the FePc. We use Vanderbilt ultrasoft pseudopotentials (GBRV) [53] with semi-core corrections. The kinetic energy cutoffs were set to 45 Ry and 270 Ry for the plane-wave expansion of the wavefunctions and of the charge density, respectively. Given the moderately large surface supercell with lattice vectors amounting to 1.77 and 2.01 nm, we sample the Brillouin zone by the Γ point. The substrate is modelled by a slab approach, including 3 NiO(001) layers. Equilibrium geometries are obtained by structural optimization of the molecule and of the topmost two NiO(001) layers. Optical spectra of the FePc/NiO(001) system, of the clean NiO(001) surface and of the gas phase FePc molecule are obtained from the 2D polarizability, which is extracted from the imaginary part of the dielectric function. This is evaluated at the independent particle (IP) level through the Kohn–Sham states and dipole moments, i.e. through the matrix elements of the commutator $[r, H]$. These calculations are done using Yambo [54], a plane wave code interfaced with Quantum ESPRESSO. As Yambo is not currently compatible with ultrasoft pseudopotentials nor the vdW-DF-C09 exchange correlation functional, these spectra are evaluated within the Perdew-Burke-Ernzerhof [55] (PBE)+U approach with norm-conserving pseudopotentials (Pseudo-Dojo [56]), from the previously determined geometry. In the evaluation of the dipole moments, the DFT + U Kohn–Sham states are used, while in a simplifying approximation, we neglect the Hubbard term in the Hamiltonian inside the commutator $[r, H]$ (not implemented in Yambo). We verified that such an approximation yields qualitatively analogue results to the full calculation ("covariant dipoles" in Yambo), at lower computational cost.

3. Results

3.1. Adsorption configurations

Before discussing interface systems, we recall a few results about FePc in the gas phase. This is an open d-shell molecule, and consistently with the literature [57] we find that its minimum energy configuration corresponds to a D_{2h} symmetry where the in-plane degeneracy of d-orbitals (d_{xz}, d_{yz}) is lifted by Jahn–Teller (JT) effect with a small distortion in the geometry with respect to the corresponding symmetric conformation (D_{4h}), with a difference in the nonequivalent Fe-N bond length of 1%. We find that the D_{2h} molecule is characterized by a lower magnetic moment on the iron atom (2.17 μ_B) with respect to the D_{4h} one (2.27 μ_B), while the difference in energy amounts to 0.25 eV. Moreover, the electronic density of states (DOS), spectra and, in particular, the occupancy of m-resolved d orbitals exhibit remarkable changes. In the following, the D_{2h} molecule is taken as a reference for comparison with the gas phase results.

We investigate the adsorption of FePc on NiO(001) by considering a $((6\,0)(3\,3))$ surface supercell, as referred to the surface magnetic unit cell as depicted in Fig. 1. Within such a supercell, the simulations explore adsorption configurations for a diluted FePc overlayer; in fact, the distance between Fe centers (17.68 Å) of nearby molecules is more than 3 Å larger than that for dense Pc layers [58,59]. In particular, in the

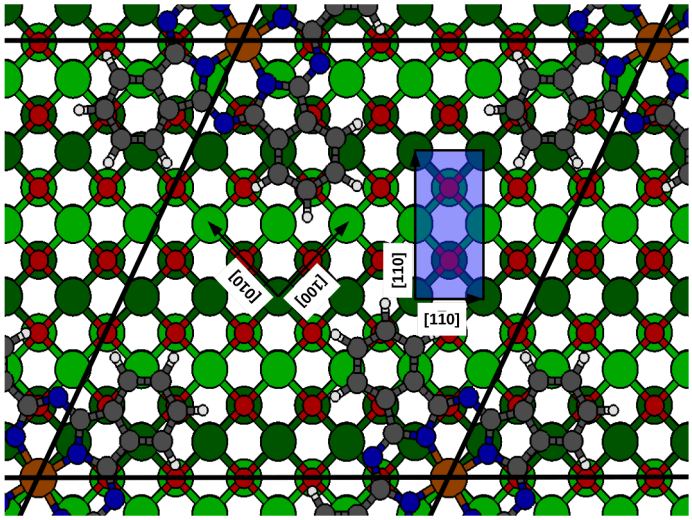

Fig. 1. Surface supercell adopted for the calculations (black line), having epitaxy matrix $((6\,0)(3\,3))$ with respect to the surface primitive cell of antiferromagnetic NiO(001) (shaded-blue). Color scheme as follows. Light and dark green: Ni atoms, according to their magnetization; Red: O; Brown: Fe; Blue: N; Dark-gray: C; Light-gray: H.

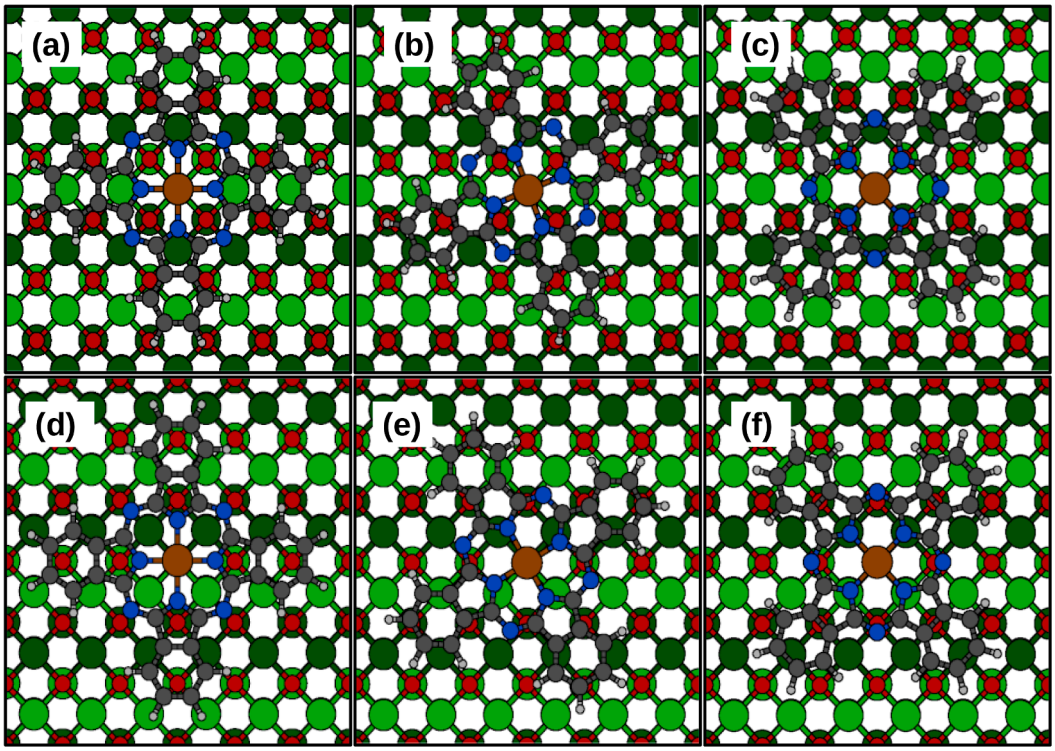

Fig. 2. Optimized geometry for FePc/NiO(001) on a Ni site (a-c) and on a O one (d-f), with optimized azimuthal angle (see text) equal to 0° (a,d), 22° (b), 31° (e), and 45° (c,f). Color scheme as in Fig. 1.

minimum energy adsorption configuration, the distance between the H of the two molecules is at least 5.73 Å. We take into account adsorption with the Fe atom of FePc on top of surface Ni and surface O atoms, and different molecular orientations, namely with a N-Fe-N axis forming with the $[1\bar{1}0]$ direction an angle of 0°, 22.5°, and 45°. For each adsorption site, we can distinguish two possible magnetic configurations for the molecule: one where the Ni atom underneath has the same spin (that we denote as ferromagnetic, "FM"), or opposite spin (antiferromagnetic, "AF") of Fe. For adsorption on the O atom, the spin of the second-layer Ni is considered, taking into account that the superexchange interaction metal-O-metal in metal oxides is stronger than the metal–metal exchange one. We report in Fig. 2 optimized structures and in Table 1 the corresponding adsorption energies, defined as the difference between the total energy of the full system and that of the clean substrate and free molecule. As shown in Table 1, we find that the O configurations are generally lower in energy than Ni ones. Moreover, configurations with the starting intermediate rotation angle of 22.5° (in Table 1 the optimized angle is reported) are generally lower in energy, with the only exception of the FM Ni case where 0° and 22.5° yield very similar energy. Considering the magnetic orientation, it is remarkable that the energy difference between the adsorption energy in AF and FM cases depends not only on the adsorption site but also strongly on the angle, proving that the coupling with the surface magnetization is also mediated by the specific positioning of the molecular macrocycle. At almost all cases, the AF coupling is preferred. The minimum energy configuration overall, above O in the AF configuration at intermediate angle, exhibits a smaller dependence on spin alignment than other cases, testifying the relevance of other kind of interactions beyond the magnetic one. For this configuration, the AF coupling may be expected following the superexchange path Fe-O-Ni at 180° [60]. This is further detailed in the section discussing magnetic properties. Coming to adsorption geometries, in the Ni configurations the molecule atoms keep the same distance of 2.92 ± 0.01 Å (average height) from the top surface layer irrespectively of the angle. Conversely, in the O configurations the Fe atom approaches the surface, causing a molecule deformation. This effect is most important in the most stable O 31° case where the Fe atom sits at 2.46 Å height from the surface, with a Fe-O distance of 2.37 Å, also pulling the N atoms at 2.65 Å (see Fig. 3(a)). The small distance between the molecule and the substrate of the O configuration at 31° approaches the typical length of the Fe-O bond (2.14 Å) in bulk FeO. The Fe-N distances amount to 1.962 Å and 1.960 Å (1.944 Å and 1.938 Å for free FePc), reducing the difference but maintaining a JT distortion that emerges in the Fe electronic densities of states (see Section 3.2 below).

Table 1
Adsorption energy for FePc/NiO(001) as a function of adsorption site and optimized angle, for FM and AF orientation of the Fe spin with respect to underlying Ni. Values in eV.

Site	Angle	E_{ads}^{FM}	E_{ads}^{AF}	$E_{ads}^{AF} - E_{ads}^{FM}$
Ni	0°	−4.39	−4.21	0.18
Ni	22°	−4.38	−4.59	−0.21
Ni	45°	−4.34	-4.51	−0.16
O	0°	−4.57	−4.70	−0.13
O	31°	−5.12	−5.18	-0.05
O	45°	−4.68	−4.71	-0.03

3.2. Electronic properties

Hereafter we focus on the most stable adsorption configuration. We discuss electronic properties by looking at the projected density of states (PDOS) reported in Fig. 4. We can observe that the lowest-unoccupied molecular orbital (LUMO) of FePc lies within the substrate bandgap, exhibiting similar characteristics as in the free molecule, see dash-dotted line in Fig. 4(a) (there, the molecule has negative spin as in the adsorbed configuration). Hence, the overall gap of the adsorbed system is reduced with respect to the pristine system. Conversely, the highest occupied molecular orbital (HOMO) lies within the valence band of NiO. A type-II interface is then formed, with an overall gap smaller than that of free FePc and of pristine NiO, as reported in Table 2. One also observes a small molecular contribution to the PDOS in correspondence of the

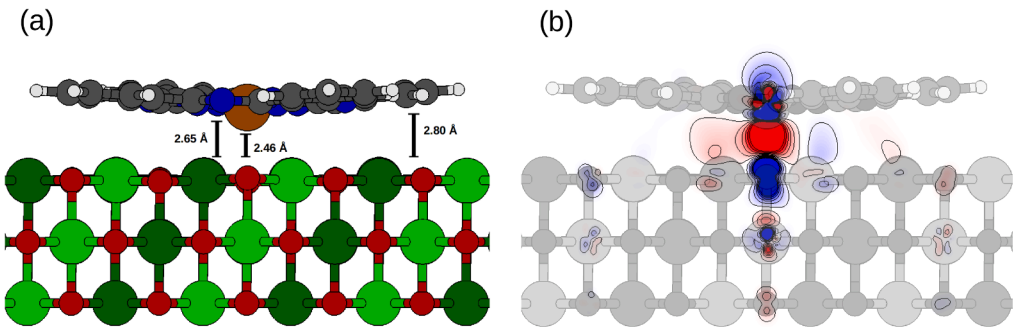

Fig. 3. (a) Side view of FePc/NiO(001) in the most stable (O 31° AF) configuration and height over the surface of the Fe atom and of the average CHN atoms (Å). (b) Spin-density variation (red: increase; blue: decrease); isolines in the range from −0.02 to 0.02 Å^{-3}.

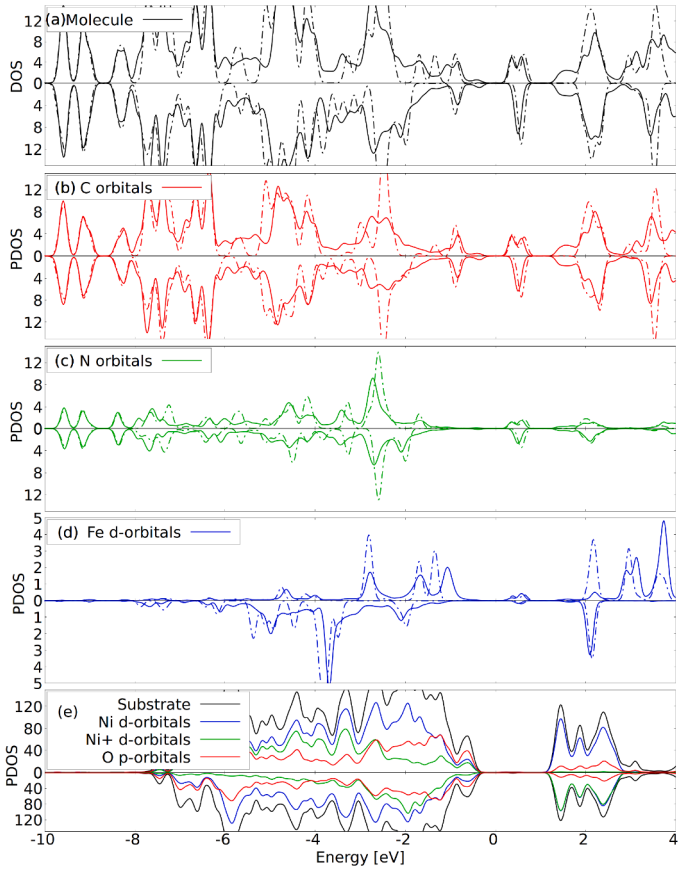

Fig. 4. Electronic PDOS of FePc/NiO(001), summed over: (a) all molecule atoms; (b) C; (c) N; (d) Fe; (e) substrate atoms. Substrate color codes: Black: all substrate atoms; Blue: all Ni atoms (*d* orbitals); Green: Ni atoms of one spin component ("Ni+", *d* orbitals); Red: O atoms (*p* orbitals). Solid/dash-dotted lines indicate adsorbed and gas phase molecules, respectively. Negative spin components are shown as negative values. All values in states/eV/cell.

Table 2
Electronic gap of the full FePc/NiO(001) system in comparison to free FePc and to the clean NiO(001) surface.

System	Spin channel	Gap (eV)
free FePc	up	1.27
free FePc	down	1.46
FePc/NiO(001)	up	0.69
FePc/NiO(001)	down	0.80
NiO(001)	up/down	1.80

valence band maximum and a substrate one in correspondence of the LUMO as a result of adsorption. Adsorption modifies the molecular levels following hybridization with substrate states to a different extent. This is most evident for Fe orbitals that are further detailed in Fig. 5. In particular, while the in-plane $d_{x^2-y^2}$ and d_{xy} orbitals only show some broadening of the peaks, the d_{xz}/d_{yz} and even more the d_{z^2} state shift and spread over wide energy ranges, evidencing a strong coupling with the surface. The LUMO and HOMO, that have mostly C character, are mildly affected but other molecular states with strong C and N weight (e.g., those around −2.5 eV) broaden significantly (Fig. 4 (b) and (c)).

3.3. Magnetic properties

We now describe the variations in the magnetic structure in the substrate and in the molecule as a result of adsorption, collected in Fig. 6. Looking to Fig. 6 for the first substrate layer, effects of the molecule on the substrate are mostly localized under the molecule. We

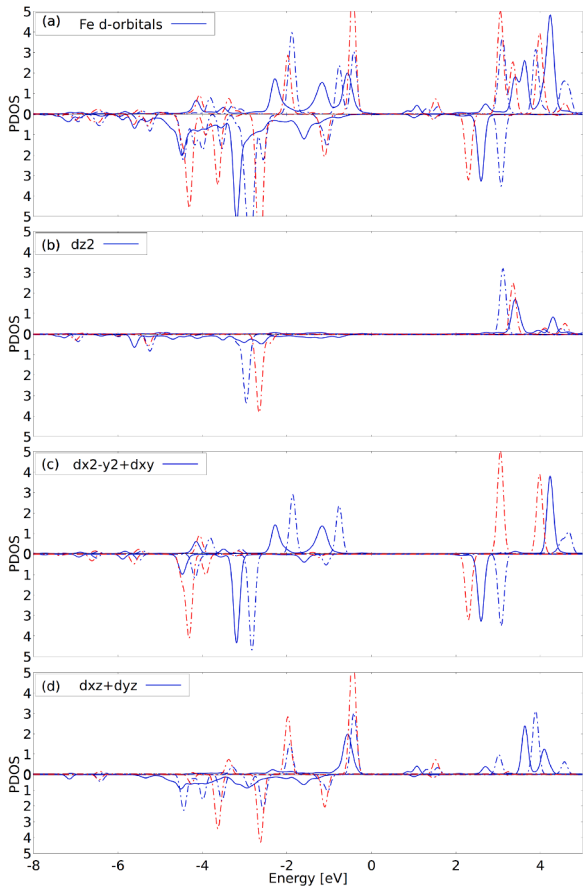

Fig. 5. Electronic PDOS on the Fe atom in FePc/NiO(001). (a) all *d* orbitals; (b) projected on d_{z^2}; (c) $d_{x^2-y^2} + d_{xy}$; (d) $d_{xz} + d_{yz}$. Blue solid/dash-dotted lines indicate adsorbed and gas phase (D_{2h}) molecules, respectively. Red dash-dotted lines indicate the gas phase molecule in the D_{4h} configuration. Negative spin components are shown as negative values. All values in states/eV/cell.

observe a lowering of the absolute value of the Ni magnetic moments below the center of the molecule up to about 30×10^{-3} μ_B ($\approx 2\%$). Simultaneously, the magnetic moment of O atoms changes by up to 10×10^{-3} μ_B, apart for the O below the iron center of the molecule, which reduces by 43×10^{-3} μ_B. This behavior can be rationalized considering the super-exchange between Ni atoms through the oxygens: in the bulk, each O atom bridges three Ni pairs [61], whereas in the surface no Ni atom is present above O, so that surface O acquire magnetization themselves and bridge surface Ni with molecule Fe, as previously pointed out for Fe-porphyrin on O-passivated magnetic metals [42]. The O atom below Fe thus participates to a Fe-O-Ni bridge, partially restoring its bulk-like non-magnetic character as evidenced by a detailed spin density difference shown in Fig. 3(b). Looking to the molecule variations in Fig. 6 (d), the main change occurs at the Fe atom which reduces its magnetic moment by 40×10^{-3} μ_B (from -2.17 to $-2.13\mu_B$). Smaller but non-negligible changes are also seen on the other atoms. In particular, the magnetic moment on the full molecule changes from -2.0 to -1.95 μ_B, while considering an average on molecule atoms excluding Fe, the magnetic moment changes from 0.172 to 0.176 μ_B. We remark that variations do not exhibit the C_2 symmetry of the molecule because of the different symmetry of the underlying substrate. In specific cases, these modifications in the magnetic moment correlate to the corresponding ones of the charge, depicted in Fig. 6 (e) and (f). Especially, there is a transfer of 0.04 electrons to the Fe atom, hence increasing the filling of the spin-minority population and reducing the magnetic moment. As for the substrate, Ni atoms exhibit a similar behavior acquiring charge and reducing their magnetic moment. Conversely, O atoms under the molecule see a decrease in electron density that is not strictly related to changes in the magnetic moments. Looking at the molecule, the C and N atoms most frequently lose electron density (with a charge displacement pattern reminiscent of JT distortion), so that overall we compute a transfer of 0.25 electrons from the molecule to the substrate, which we attribute to an average displacement of the molecular orbitals towards the substrate. .

3.4. Optical properties

We study the optical absorption spectrum of FePc/NiO(001) in the minimum energy adsorption configuration. As a preliminary step, we

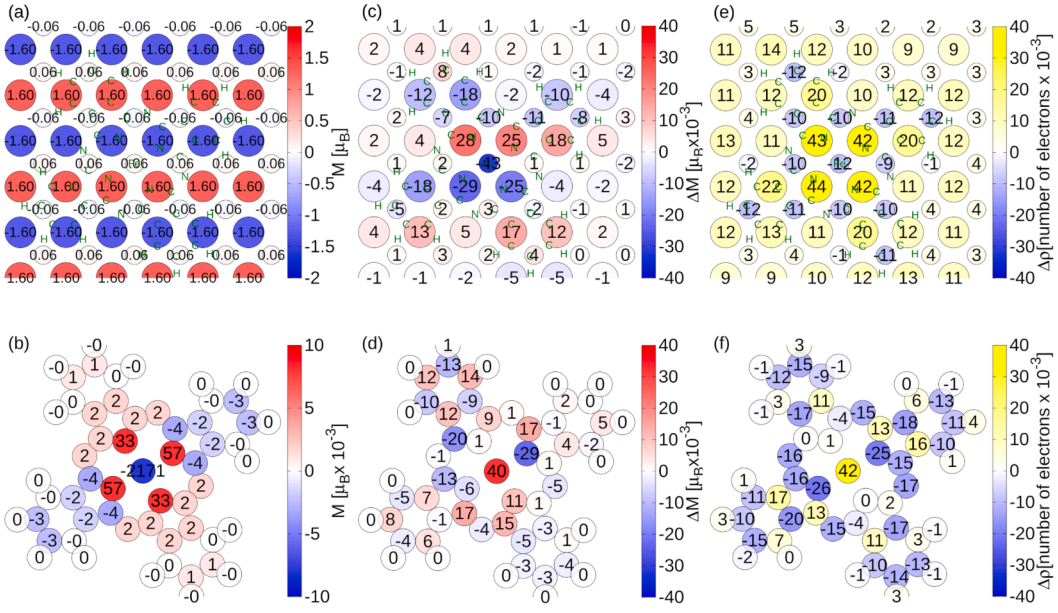

Fig. 6. Values of the atomic magnetic moments for the clean surface NiO(001) (a) and the isolated molecule FePc (b); variations in the atomic magnetic moments for FePc/NiO(001), with respect to the isolated systems, on the surface (c) and on the molecule (d). Corresponding variations in the electron density (e)-(f) (positive = increase in electron population). The position of molecule atoms is marked by green letters in panels (a), (c), and (e).

Table 3
Fe, C and N orbital contributions to the first peaks conduction levels in the FePc gas-phase optical absorption spectrum (the relative spin channels of the optical transition is also underlined).

Energy (eV)	Valence	Conduction	Fe (%)	C (%)	N (%)	spin
1.29	HOMO	LUMO	4	72	24	up
1.46	HOMO	LUMO	2	68	31	down
1.47	HOMO	LUMO + 1	2	68	31	down
1.53	HOMO	LUMO + 1	6	63	32	up

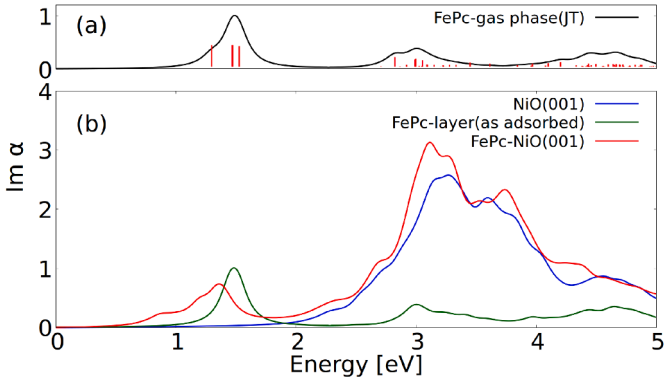

Fig. 7. Optical absorption spectra (independent particle): (a) gas-phase molecular polarizability (black line) and respective transitions (red sticks); (b) polarizability of: NiO(001) (blue), FePc/NiO(001) (red), and FePc-layer as in FePc/NiO(001) (green). The two spectra (a) and (b) are separately normalized to the molecular peak at ≈ 1.5 eV. Spectra are broadened by 0.01 eV.

analyse the free molecule. We average optical spectra at normal incidence among two orthogonal in-plane light polarizations and report the results in Fig. 7(a). Looking at the first peak, we can identify four main contributions (sticks in the figure, two nearly degenerate) in the interval energy from 1.29 to 1.53 eV. Compared to experimental results where the low energy peaks are observed at 1.73, 1.96 and 2.18 eV [62], these values underestimate the excitation energy as a result of the independent particle (DFT + U) approach (hybrid functionals would give a larger HOMO–LUMO gap [52]). These identified contributions (Table 3) are characterized by transitions from the HOMO level, having C nature, to unoccupied levels having also contributions from the Fe (≈ 2 −5%) and N (≈ 30%) orbitals, i.e., with a consequent accumulation of electron density in the magnetic center of the molecule during the excitation. In particular, looking at the Fe atom (magnetic moment equal to $-2.16\ \mu_B$ to reflect the antiferromagnetic coupling upon adsorption), all transitions contribute to a different extent into filling states having d_{xz}/d_{yz} symmetry. For the transitions at 1.29 and 1.53 eV ("up spin", minority channel) there is an increase of the number of spin-minority electrons and a decrease of the Fe magnetic moment. Conversely, the nearly degenerate transitions at 1.46/1.47 eV ("down spin", majority channel) increase the number of majority electrons. Overall, given the largest contribution of Fe in minority spin transitions, a reduction of the Fe magnetic moment could be expected in this IP approach built upon a DFT $+U$ ground state, hinting to a small coupling between the optical excitation and the spin properties of the molecule.

Spectra for FePc/NiO(001) system are reported in Fig. 7 (b) and compared to the ones of the clean NiO(001) substrate and of a free-standing FePc layer. This highlights a set of peaks appearing for the adsorbed system at energies below the absorption edge both of NiO and of FePc. Indeed, these peaks are related to the interface, i.e., to effects of hybridization between the molecular orbitals and the substrate ones as discussed above. In detail, we identify contributions at 1.19, 1.33, 1.36, and 1.41 eV analogue to the free-molecule ones. These are transitions from FePc valence states of C nature, to empty molecular states with mainly C (62%) and N contributions (25%) and a smaller contribution from the Fe atom (2% in the minority spin channel and 1% in the majority spin channel). For the latter, we hence compute a filling of the empty d_{xz}/d_{yz} in the minority spin channel that reflects the above analysis for the free molecule, with the differences that energy levels are now shifted toward lower energies and the contributions from the Fe atom to the conduction levels are smaller. Additionally, we single out a secondary peak around 0.9 eV that is ≈ 1/7 as intense as the above structures. This is given by transitions where the conduction state still corresponds to molecular LUMO/LUMO + 1 orbitals, whereas the valence state is mostly of substrate origin, with a small molecular contribution (C at 3%) corresponding to the interface state at ≈ −0.4 eV in Fig. 4(a).

4. Conclusions

In this study we have characterized theoretically the electronic interface states between a paradigmatic organo-metallic molecule and transition-metal monoxide. We have identified the minimum energy adsorption configuration of FePc on NiO(001), noticing a remarkable energy dependence on the adsorption site and orientation of the molecule. In particular, specific adsorption angles enable a molecular lock-in into the surface lattice, with the Fe atom pulled towards a surface O, and viceversa. O-mediated super-exchange between Fe and subsurface Ni favors an antiferromagnetic alignment between their respective spin. We have shown that molecular states hybridize with substrate ones, especially those involving the out-of-plane Fe *d* orbitals.

Local variations of magnetization and charges, both at the molecule and the substrate, occur as a result of interaction. In particular we observe a reduction of the Fe and Ni magnetic moments, with electron transfer from molecule to substrate and from O to Ni atoms within the first surface layer. Optical spectra computed at the independent particle level show that the first transitions of the free molecule are also present for adsorbed ones, with additional structures at lower energy in the latter, corresponding to transitions from hybrid states of mostly substrate character to molecular ones. Transitions having a final state with Fe contribution underline a possible mechanism to alter its magnetic configuration through light.

CRediT authorship contribution statement

Marco Marino: Conceptualization, Formal analysis, Investigation, Validation, Visualization, Writing - original draft, Writing - review & editing. **Elena Molteni:** Conceptualization, Formal analysis, Investigation, Validation, Writing - original draft, Writing - review & editing. **Simona Achilli:** Investigation, Validation, Writing - review & editing. **Guido Fratesi:** Conceptualization, Investigation, Validation, Visualization, Writing - original draft, Writing - review & editing.

Declaration of Competing Interest

The authors declare that they have no known competing financial interests or personal relationships that could have appeared to influence the work reported in this paper.

Data availability

Data will be made available on request.

Acknowledgments

This work was supported by the European Union's Horizon 2020 Research and Innovation programme under grant agreement No. 964396 FET-Open SINFONIA (Selectively activated INFOrmation technology by hybrid Organic Interfaces). We acknowledge the CINECA award under the ISCRA initiative (grants IscrC-HOAMI-HP10CJW8ZE,

IscrB-ORGAFINT-HP10BC1AM9), for the availability of high performance computing resources and support.

References

[1] V.K. Joshi, Spintronics: A contemporary review of emerging electronics devices, Engineering Science and Technology, an International Journal 19 (3) (2016) 1503–1513, https://doi.org/10.1016/j.jestch.2016.05.002.

[2] J.R. Hortensius, D. Afanasiev, M. Matthiesen, R. Leenders, R. Citro, A.V. Kimel, R. V. Mikhaylovskiy, B.A. Ivanov, A.D. Caviglia, Coherent spin-wave transport in an antiferromagnet, Nat. Phys. 17 (2021) 1001–1006, https://doi.org/10.1038/s41567-021-01290-4.

[3] O. Gomonay, T. Jungwirth, J. Sinova, Concepts of antiferromagnetic spintronics (phys. status solidi rrl 4/2017), physica status solidi (RRL), Rapid Res. Lett. 11 (4) (2017) 1770319, https://doi.org/10.1002/pssr.201770319.

[4] S.M. Rezende, A. Azevedo, R.L. Rodríguez-Suárez, Introduction to antiferromagnetic magnons, J. Appl. Phys. 126 (2019), 151101, https://doi.org/10.1063/1.5109132.

[5] V. Baltz, A. Manchon, M. Tsoi, T. Moriyama, T. Ono, Y. Tserkovnyak, Antiferromagnetic spintronics, Rev. Mod. Phys. 90 (2018), 015005, https://doi.org/10.1103/RevModPhys.90.015005.

[6] D. Xiong, Y. Jiang, K. Shi, A. Du, Y. Yao, Z. Guo, D. Zhu, K. Cao, S. Peng, W. Cai, D. Zhu, W. Zhao, Antiferromagnetic spintronics: An overview and outlook, Fundamental Res. 2 (4) (2022) 522–534, https://doi.org/10.1016/j.fmre.2022.03.016.

[7] I. Žutić, J. Fabian, S. Das Sarma, Spintronics: Fundamentals and applications, Rev. Mod. Phys. 76 (2004) 323–410, https://doi.org/10.1103/RevModPhys.76.323.

[8] W. Naber, S. Faez, W. van der Wiel, Organic spintronics, J. Phys. D: Appl. Phys. 24 (2007) R205, https://doi.org/10.1088/0022-3727/40/12/R01.

[9] S. Sanvito, Molecular spintronics, Chemical Society reviews 40 (6) (2011) 3336–3355, https://doi.org/10.1039/c1cs15047b.

[10] D.L. Esteras, A. Rybakov, A.M. Ruiz, J.J. Baldoví, Magnon straintronics in the 2D van der Waals ferromagnet CrSBr from first-principles, Nano Lett. 22 (2022) 8771–8778, https://doi.org/10.1021/acs.nanolett.2c02863.

[11] K.S. Kumar, M. Ruben, Sublimable spin-crossover complexes: From spin-state switching to molecular devices, Angew. Chem. Int. Ed. 60 (14) (2021) 7502–7521, https://doi.org/10.1002/anie.201911256.

[12] E. Coronado, Molecular magnetism: from chemical design to spin control in molecules, materials and devices, Nat. Rev. Mater. 5 (2020) 87–104, https://doi.org/10.1038/s41578-019-0146-8.

[13] A.M. Serra, A. Dhingra, M.C. Asensio, J.A. Real, J.F.S. Royo, Surface stabilisation of the high-spin state of fe(ii) spin-crossover complexes, Phys. Chem. Chem. Phys. 25 (2023) 14736–14741, https://doi.org/10.1039/D3CP00863K.

[14] F. Djeghloul, F. Ibrahim, M. Cantoni, M. Bowen, L. Joly, S. Boukari, P. Ohresser, F. Bertran, P. Le Fèvre, P. Thakur, F. Scheurer, T. Miyamachi, R. Mattana, P. Seneor, A. Jaafar, C. Rinaldi, S. Javaid, J. Arabski, J.P. Kappler, W. Wulfhekel, N.B. Brookes, R. Bertacco, A. Taleb-Ibrahimi, M. Alouani, E. Beaurepaire, W. Weber, Direct observation of a highly spin-polarized organic spinterface at room temperature, Sci Rep 3 (2013) 1272, https://doi.org/10.1038/srep01272.

[15] A. Lodi Rizzini, C. Krull, T. Balashov, J.J. Kavich, A. Mugarza, P.S. Miedema, P. K. Thakur, V. Sessi, S. Klyatskaya, M. Ruben, S. Stepanow, P. Gambardella, Coupling single molecule magnets to ferromagnetic substrates, Phys. Rev. Lett. 107 (2011), 177205, https://doi.org/10.1103/PhysRevLett.107.177205.

[16] A. Kumar, Advances in tetrapyrrole complexes spin interfaces, Materials Today: Proceedings 37 (2021) 2858–2863, international Conference on Newer Trends and Innovation in Mechanical Engineering: Materials Science. doi:https://doi.org/10.1016/j.matpr.2020.08.661.

[17] M. Cinchetti, V.A. Dediu, L.E. Hueso, Activating the molecular spinterface, Nat. Mater. 16 (2017) 507–515, https://doi.org/10.1038/nmat4902.

[18] H. Meer, O. Gomonay, A. Wittmann, M. Kläui, Antiferromagnetic insulatronics: Spintronics in insulating 3d metal oxides with antiferromagnetic coupling, Appl. Phys. Lett. 122 (8) (2023), 080502, https://doi.org/10.1063/5.0135079.

[19] J. Kune, V.I. Anisimov, S.L. Skornyakov, A.V. Lukoyanov, D. Vollhardt, Nio: Correlated band structure of a charge-transfer insulator, Phys. Rev. Lett. 99 (2007), 156404, https://doi.org/10.1103/PhysRevLett.99.156404.

[20] M.-S. Liao, S. Scheiner, Electronic structure and bonding in metal phthalocyanines, Metal=Fe Co, Ni, Cu, Zn, Mg, J. Chem. Phys. 114 (2001) 9780–9791, https://doi.org/10.1063/1.1367374.

[21] J.M. Gottfried, Surface chemistry of porphyrins and phthalocyanines, Surf. Sci. Rep. 70 (2015) 259–379, https://doi.org/10.1016/j.surfrep.2015.04.001.

[22] T. Kroll, R. Kraus, R. Schönfelder, V.Y. Aristov, O.V. Molodtsova, P. Hoffmann, M. Knupfer, Transition metal phthalocyanines: Insight into the electronic structure from soft x-ray spectroscopy, J. Chem. Phys. 137 (5) (2012), 054306, https://doi.org/10.1063/1.4738754.

[23] T.M. Willey, M. Bagge-Hansen, J.R.I. Lee, R. Call, L. Landt, T. van Buuren, C. Colesniuc, C. Monton, I. Valmianski, I.K. Schuller, Electronic structure differences between H2-, Fe-, Co-, and Cu-phthalocyanine highly oriented thin films observed using NEXAFS spectroscopy, J. Chem. Phys. 139 (3) (2013), 034701, https://doi.org/10.1063/1.4811487.

[24] A. Franco-Cañellas, S. Duhm, A. Gerlach, F. Schreiber, Binding and electronic level alignment of π) conjugated systems on metals, Rep. Prog. Phys. 83 (6) (2020), 066501, https://doi.org/10.1088/1361-6633/ab7a42.

[25] K. Shen, B. Narsu, G. Ji, H. Sun, J. Hu, Z. Liang, X. Gao, H. Li, Z. Li, B. Song, Z. Jiang, H. Huang, J.W. Wells, F. Song, On-surface manipulation of atom substitution between cobalt phthalocyanine and the cu(111) substrate, RSC Adv. 7 (2017) 13827–13835, https://doi.org/10.1039/C7RA00636E.

[26] H. Peisert, J. Uihlein, F. Petraki, T. Chassé, Charge transfer between transition metal phthalocyanines and metal substrates: The role of the transition metal, Journal of Electron Spectroscopy and Related Phenomena 204 (2015) 49–60, organic Electronics. doi:https://doi.org/10.1016/j.elspec.2015.01.005.

[27] J. Åhlund, J. Schnadt, K. Nilson, E. Göthelid, J. Schiessling, F. Besenbacher, N. Mårtensson, C. Puglia, The adsorption of iron phthalocyanine on graphite: A scanning tunnelling microscopy study, Surf. Sci. 601 (17) (2007) 3661–3667, https://doi.org/10.1016/j.susc.2007.06.008.

[28] M. Wagner, F. Calcinelli, A. Jeindl, M. Schmid, O.T. Hofmann, U. Diebold, Adsorption configurations of Co-phthalocyanine on In2O3(111), Surf. Sci. 722 (2022), 122065, https://doi.org/10.1016/j.susc.2022.122065.

[29] R. Karstens, T. Chassé, H. Peisert, Interface interaction of transition metal phthalocyanines with strontium titanate (100), Beilstein, Journal of Nanotechnology 12 (2021) 485–496, https://doi.org/10.3762/bjnano.12.39.

[30] L. Liu, W. Zhang, P. Guo, K. Wang, J. Wang, H. Qian, I. Kurash, C.-H. Wang, Y.-W. Yang, F. Xu, A direct fe-o coordination at the fepc/moox interface investigated by xps and nexafs spectroscopies, Phys. Chem. Chem. Phys. 17 (2015) 3463–3469, https://doi.org/10.1039/C4CP04199B.

[31] R. Karstens, M. Glaser, A. Belser, D. Balle, M. Polek, R. Ovsyannikov, E. Giangrisostomi, T. Chassé, H. Peisert, FePc and FePcF16 on Rutile TiO2(110) and (100): Influence of the Substrate Preparation on the Interaction Strength, Molecules 24 (2019) 4579, https://doi.org/10.3390/molecules24244579.

[32] T. Schmitt, P. Ferstl, L. Hammer, M.A. Schneider, J. Redinger, Adsorption and intermolecular interaction of cobalt phthalocyanine on coo(111) ultrathin films: An stm and dft study, J. Phys. Chem. C 121 (5) (2017) 2889–2895, https://doi.org/10.1021/acs.jpcc.6b12337.

[33] M. Glaser, H. Peisert, H. Adler, M. Polek, J. Uihlein, P. Nagel, M. Merz, S. Schuppler, T. Chassé, Transition-metal phthalocyanines on transition-metal oxides: Iron and cobalt phthalocyanine on epitaxial MnO and TiOx films, J. Phys. Chem. C 119 (49) (2015) 27569–27579, https://doi.org/10.1021/acs.jpcc.5b09612.

[34] Z. Xu, J. Liu, S. Hou, Y. Wang, Manipulation of molecular spin state on surfaces studied by scanning tunneling microscopy, Nanomaterials 10 (2020) 2393, https://doi.org/10.3390/nano10122393.

[35] I. Cojocariu, S. Carlotto, H.M. Sturmeit, G. Zamborlini, M. Cinchetti, A. Cossaro, A. Verdini, L. Floreano, M. Jugovac, P. Puschnig, C. Piamonteze, M. Casarin, V. Feyer, C.M. Schneider, Ferrous to ferric transition in fe-phthalocyanine driven by NO2 exposure, Chem.- A Eur. J. 27 (10) (2021) 3526–3535, https://doi.org/10.1002/chem.202004932.

[36] B. de la Torre, M. Švec, P. Hapala, J. Redondo, O. Krejčí, R. Lo, D. Manna, A. Sarmah, D. Nachtigallová, J. Tuček, P. Błoński, M. Otyepka, R. Zbořil, P. Hobza, P. Jelínek, Non-covalent control of spin-state in metal-organic complex by positioning on N-doped graphene, Nat. Commun. 9 (2018) 2831, https://doi.org/10.1038/s41467-018-05163-y.

[37] P. Willke, T. Bilgeri, X. Zhang, Y. Wang, C. Wolf, H. Aubin, A. Heinrich, T. Choi, Coherent spin control of single molecules on a surface, ACS Nano 15 (2021) 17959–17965, https://doi.org/10.1021/acsnano.1c06394.

[38] D.M. Janas, A. Windischbacher, M.S. Arndt, M. Gutnikov, L. Sternemann, D. Gutnikov, T. Willershausen, J.E. Nitschke, K. Schiller, D. Baranowski, V. Feyer, I. Cojocariu, K. Dave, P. Puschnig, M. Stupar, S. Ponzoni, M. Cinchetti, G. Zamborlini, Metalloporphyrins on oxygen-passivated iron: Conformation and order beyond the first layer, Inorg. Chim. Acta 557 (2023), 121705, https://doi.org/10.1016/j.ica.2023.121705.

[39] H.M. Sturmeit, I. Cojocariu, A. Windischbacher, P. Puschnig, C. Piamonteze, M. Jugovac, A. Sala, C. Africh, G. Comelli, A. Cossaro, A. Verdini, L. Floreano, M. Stredansky, E. Vesselli, C. Hohner, M. Kettner, J. Libuda, C.M. Schneider, G. Zamborlini, M. Cinchetti, V. Feyer, Room-temperature on-spin-switching and tuning in a porphyrin-based multifunctional interface, Small 17 (50) (2021) 2104779, https://doi.org/10.1002/smll.202104779.

[40] C. Wäckerlin, D. Chylarecka, A. Kleibert, K. Müller, C. Iacovita, F. Nolting, T.A. Jung, N. Ballav, Controlling spins in adsorbed molecules by a chemical switch., Nature Communications 1 (61) (2010) 2041–1723. doi:https://doi.org/10.1038/ncomms1057.

[41] A. Windischbacher, P. Puschnig, Computational study on the adsorption of small molecules to surface-supported ni-porphyrins, Inorg. Chim. Acta 558 (2023), 121719, https://doi.org/10.1016/j.ica.2023.121719.

[42] M. Bernien, J. Miguel, C. Weis, M.E. Ali, J. Kurde, B. Krumme, P.M. Panchmatia, B. Sanyal, M. Piantek, P. Srivastava, K. Baberschke, P.M. Oppeneer, O. Eriksson, W. Kuch, H. Wende, Tailoring the nature of magnetic coupling of fe-porphyrin molecules to ferromagnetic substrates, Phys. Rev. Lett. 102 (2009), 047202, https://doi.org/10.1103/PhysRevLett.102.047202.

[43] X. Zhang, P.S. Costa, J. Hooper, D.P. Miller, A.T. N'Diaye, S. Beniwal, X. Jiang, Y. Yin, P. Rosa, L. Routaboul, M. Gonidec, L. Poggini, P. Braunstein, B. Doudin, X. Xu, A. Enders, E. Zurek, P.A. Dowben, Locking and unlocking the molecular spin crossover transition, Adv. Mater. 29 (39) (2017) 1702257, https://doi.org/10.1002/adma.201702257.

[44] B. Himmetoglu, A. Floris, S. de Gironcoli, M. Cococcioni, Hubbard-corrected DFT energy functionals: The LDA+U description of correlated systems, Int. J. Quantum Chem. 114 (2014) 14–49, https://doi.org/10.1002/qua.24521.

[45] P. Giannozzi, S. Baroni, N. Bonini, M. Calandra, R. Car, C. Cavazzoni, D. Ceresoli, G.L. Chiarotti, M. Cococcioni, I. Dabo, A. Dal Corso, S. de Gironcoli, S. Fabris, G. Fratesi, R. Gebauer, U. Gerstmann, C. Gougoussis, A. Kokalj, M. Lazzeri, L. Martin-Samos, N. Marzari, F. Mauri, R. Mazzarello, S. Paolini, A. Pasquarello, L. Paulatto, C. Sbraccia, S. Scandolo, G. Sclauzero, A.P. Seitsonen, A. Smogunov,

P. Umari, R.M. Wentzcovitch, Quantum ESPRESSO: a modular and open-source software project for quantum simulations of materials, J. Phys.: Condens. Mat. 21 (2009), 395502, https://doi.org/10.1088/0953-8984/21/39/395502.
[46] P. Giannozzi, O. Andreussi, T. Brumme, O. Bunau, M.B. Nardelli, M. Calandra, R. Car, C. Cavazzoni, D. Ceresoli, M. Cococcioni, N. Colonna, I. Carnimeo, A.D. Corso, S. de Gironcoli, P. Delugas, R.A.D. Jr, A. Ferretti, A. Floris, G. Fratesi, G. Fugallo, R. Gebauer, U. Gerstmann, F. Giustino, T. Gorni, J. Jia, M. Kawamura, H.-Y. Ko, A. Kokalj, E. Küçükbenli, M. Lazzeri, M. Marsili, N. Marzari, F. Mauri, N.L. Nguyen, H.-V. Nguyen, A.O. de-la Roza, L. Paulatto, S. Poncé, D. Rocca, R. Sabatini, B. Santra, M. Schlipf, A.P. Seitsonen, A. Smogunov, I. Timrov, T. Thonhauser, P. Umari, N. Vast, X. Wu, S. Baroni, Advanced capabilities for materials modelling with quantum espresso, J. Phys.: Condensed Matter 29 (2017) 465901. doi: https://doi.org/10.1088/1361-648X/aa8f79.
[47] V. Cooper, Van der Waals density functional: An appropriate exchange functional, Phys. Rev. B 81 (2010), 161104, https://doi.org/10.1103/physrevb.81.161104.
[48] K. Lee, E.D. Murray, L. Kong, B.I. Lundqvist, D.C. Langreth, Higher-accuracy van der Waals density functional, Phys. Rev. B 82 (2010), 081101, https://doi.org/10.1103/PhysRevB.82.081101.
[49] C. Rödl, F. Fuchs, J. Furthmüller, F. Bechstedt, Quasiparticle band structures of the antiferromagnetic transition-metal oxides MnO, FeO, CoO, and NiO, Phys. Rev. B 79 (2009), 235114, https://doi.org/10.1103/PhysRevB.79.235114.
[50] A. Schrön, F. Bechstedt, Spin-dependent properties and images of MnO, FeO, CoO, and NiO(001) surfaces, Phys. Rev. B 92 (2015), 165112, https://doi.org/10.1103/PhysRevB.92.165112.
[51] B. Brena, C. Puglia, M. de Simone, M. Coreno, K. Tarafder, V. Feyer, R. Banerjee, E. Göthelid, B. Sanyal, P.M. Oppeneer, O. Eriksson, Valence-band electronic structure of iron phthalocyanine: An experimental and theoretical photoelectron spectroscopy study, J. Chem. Phys. 134 (2011), 074312, https://doi.org/10.1063/1.3554212.
[52] I.E. Brumboiu, S. Haldar, J. Lüder, O. Eriksson, H.C. Herper, B. Brena, B. Sanyal, Influence of electron correlation on the electronic structure and magnetism of transition-metal phthalocyanines, J. Chem. Theory Comput. 12 (2016) 1772–1785, https://doi.org/10.1021/acs.jctc.6b00091.
[53] K.F. Garrity, J.W. Bennett, K.M. Rabe, D. Vanderbilt, Pseudopotentials for high-throughput DFT calculations, Comput. Mater. Sci. 81 (2014) 446–452, https://doi.org/10.1016/j.commatsci.2013.08.053.
[54] D. Sangalli, et al., Many-body perturbation theory calculations using the yambo code, J. Phys.: Condens. Matter 31 (2019), 325902, https://doi.org/10.1088/1361-648x/ab15d0.
[55] J.P. Perdew, K. Burke, M. Ernzerhof, Generalized gradient approximation made simple, Phys. Rev. Lett. 77 (1996) 3865, https://doi.org/10.1103/PhysRevLett.77.3865.
[56] M.J. van Setten, M. Giantomassi, E. Bousquet, M. Verstraete, D.R. Hamann, X. Gonze, G.-M. Rignanese, The pseudodojo: Training and grading a 85 element optimized norm-conserving pseudopotential table, Comput. Phys. Commun. 226 (2018) 39–54, https://doi.org/10.1016/j.cpc.2018.01.012.
[57] M.C.M. O'Brien, C.C. Chancey, The Jahn-Teller effect: An introduction and current review, Am. J. Phys. 61 (1993) 688–697, https://doi.org/10.1119/1.17197.
[58] G. Fratesi, D. Paoloni, L. Persichetti, L. Camilli, A. Caporale, A. Baby, D. Cvetko, G. Kladnik, A. Morgante, A. Ruocco, Spontaneous transmetalation at the znpc/al (100) interface, Inorg. Chim. Acta 559 (2024), 121790, https://doi.org/10.1016/j.ica.2023.121790.
[59] I. Cojocariu, A. Windischbacher, D. Baranowski, M. Jugovac, R.C. d. C. Ferreira, J. Doležal M. Švec, J.M. Zamalloa-Serrano, M. Tormen, L. Schio, L. Floreano, J. Dreiser, P. Puschnig, V. Feyer, C.M. Schneider, Surface-mediated spin locking and thermal unlocking in a 2D molecular array, Advanced Science 10 (22) (2023) 2300223. doi:https://doi.org/10.1002/advs.202300223.
[60] P.W. Anderson, Antiferromagnetism. theory of superexchange interaction, Phys. Rev. 79 (1950) 350–356. doi:https://doi.org/10.1103/PhysRev.79.350.
[61] M.I.K.R. Logemann, A.N. Rudenko, A. Kirilyuk, Exchange interactions in transition metal oxides: the role of oxygen spin polarization, J. Phys.: Condens. Matter 29 (33) (2017), 335801, https://doi.org/10.1088/1361-648X/aa7b00.
[62] A.B. Djurišić, C.Y. Kwong, T.W. Lau, Z.T. Liu, H.S. Kwok, L.S.M. Lam, W.K. Chan, Spectroscopic ellipsometry of metal phthalocyanine thin films, Appl. Opt. 42 (31) (2003) 6382–6387, https://doi.org/10.1364/AO.42.006382.